5614–5624 *Nucleic Acids Research, 2017, Vol. 45, No. 9* *Published online 6 April 2017*
doi: 10.1093/nar/gkx215

Achieving large dynamic range control of gene expression with a compact RNA transcription–translation regulator

Alexandra M. Westbrook[1] and Julius B. Lucks[2,*]

[1]Robert F. Smith School of Chemical and Biomolecular Engineering, Cornell University, Ithaca, NY 14853, USA and [2]Department of Chemical and Biological Engineering, Northwestern University, Evanston, IL 60208, USA

Received May 24, 2016; Revised March 18, 2017; Editorial Decision March 21, 2017; Accepted March 23, 2017

ABSTRACT

RNA transcriptional regulators are emerging as versatile components for genetic network construction. However, these regulators suffer from incomplete repression in their OFF state, making their dynamic range less than that of their protein counterparts. This incomplete repression causes expression leak, which impedes the construction of larger synthetic regulatory networks as leak propagation can interfere with desired network function. To address this, we demonstrate how naturally derived antisense RNA-mediated transcriptional regulators can be configured to regulate both transcription and translation in a single compact RNA mechanism that functions in *Escherichia coli*. Using *in vivo* gene expression assays, we show that a combination of transcriptional termination and ribosome binding site sequestration increases repression from 85% to 98%, or activation from 10-fold to over 900-fold, in response to cognate antisense RNAs. We also show that orthogonal repressive versions of this mechanism can be created through engineering minimal antisense RNAs. Finally, to demonstrate the utility of this mechanism, we use it to reduce network leak in an RNA-only cascade. We anticipate these regulators will find broad use as synthetic biology moves beyond parts engineering to the design and construction of more sophisticated regulatory networks.

INTRODUCTION

RNAs are now understood to play broad regulatory roles across the cell (1). As such, synthetic biologists have sought to use these versatile natural systems to create a diverse array of parts that can regulate many aspects of gene expression including transcription (2–4), translation (5,6) and mRNA degradation (7–9). Antisense-mediated RNA transcriptional regulators are particularly versatile because they regulate RNA synthesis as a function of an RNA input and thus can be used to create RNA-only genetic networks (2,10). RNA genetic networks have many potential advantages over protein-based networks including the possibility of leveraging advances in RNA folding algorithms and design rules for part design (5,11,12) and their natural fast dynamics (10).

Despite these advantages, RNA transcriptional regulators still suffer from low dynamic range, the ratio of maximum (ON) to minimum (OFF) signal, in comparison to protein-based regulators. This can be caused by excess signal in the OFF state, causing networks that contain these regulators to be disrupted by low, transient amounts of gene expression signal called network leak. Leak can propagate through the network causing it to function incorrectly, for example by causing a network to express a gene when repression is desired. Previous research has focused on reducing leak to diminish undesired effects, for example by using a recombinase to control gene availability in a multigene network to construct a digital switch biosensor (13). However, low dynamic range still remains a significant barrier to using RNA transcriptional repressors in large genetic networks. While there has been progress in creating RNA translational activators with low leak (5), there is still room for improvement in RNA translational repressors (RNA IN/OUT, 90% (10-fold) repression (14)), RNA transcriptional repressors (pT181 and variants, 85% (6-fold) repression (2)) and RNA transcriptional activators (Small transcription activating RNAs, 90-fold activation (3)). Thus, an important challenge for RNA engineering is to improve the dynamic range of RNA regulators so that they can be more effective as elements of synthetic genetic networks.

While there has been great progress in improving the dynamic range of RNA regulators by engineering mechanisms that control a single gene expression process (3,4,15), only several studies have explored the idea of engineering multiple genetic control processes for tighter regulation (16–18). Specifically, Morra *et al.* recently combined transcriptional and translational control with two distinct

*To whom correspondence should be addressed. Tel: +1 847 467 2943; Fax: +1 847 491 3728; Email: jblucks@northwestern.edu

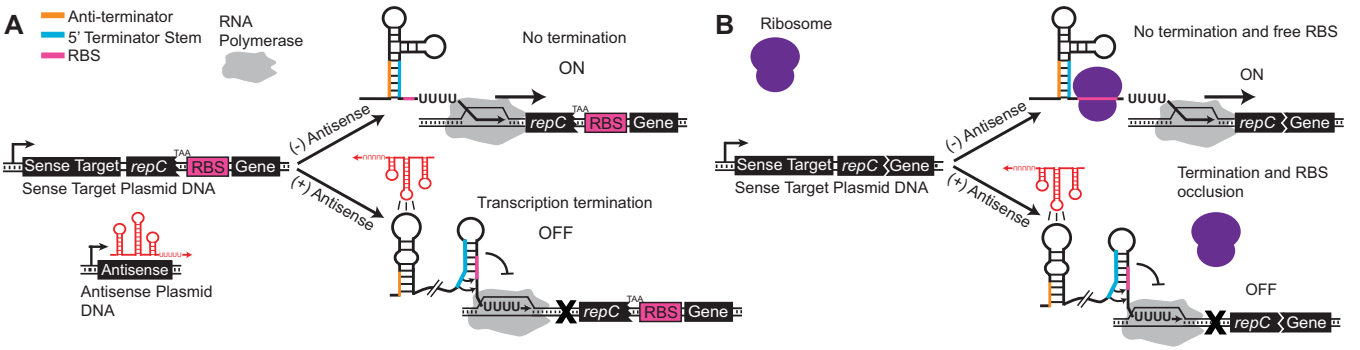

Figure 1. Schematic of the transcriptional pT181 repression mechanism (**A**) and the proposed pT181 dual transcription/translation repression mechanism (**B**). The pT181 attenuator sense target sequence resides in the 5′ untranslated region and regulates the expression of a downstream gene. The natural attenuator encoded in plasmid pT181 regulates the expression of the repC gene (30). For the transcriptional fusion, a 96 nt fragment of the *repC* gene ending in a stop codon, TAA, is included after the attenuator sequence (37) and before a ribosome binding site (RBS) and the regulated gene of interest. For the dual control/translational fusion,12 nt of the *repC* gene is included and is translationally fused to the regulated gene of interest. In the absence of antisense RNA (red), the attenuator folds such that the anti-terminator sequence (orange) sequesters the 5′ region of the terminator stem (blue), preventing terminator formation and allowing transcription elongation by RNA polymerase (gray). Thus, in the absence of antisense RNA, the attenuator is transcriptionally ON. In the dual control/translational fusion, this structure also contains an exposed ribosome binding site (RBS) for the gene of interest, which allows ribosomes (purple) to bind and translate the mRNA. When antisense RNA is present, its kissing hairpin interaction with the attenuator sequesters the anti-terminator, thus allowing terminator formation, which prevents downstream transcription. Thus, in the presence of antisense RNA, the attenuator is transcriptionally OFF. The dual control version is both transcriptionally and translationally off in this case due to the added effect of RBS occlusion by the terminator hairpin. Sequences and structures for the dual control attenuator are shown in Supplementary Figure S8.

mechanisms—inducible promoters and orthogonal translational riboswitches—to achieve tight control of fluorescent proteins (16). Horbal and Luzhetskyy also recently used a similar approach to control pamamycin production in *Streptomyces albus* (17). Using RNA engineering strategies, Liu *et al.* pursued a different approach by combining RNA-mediated translation regulators with leader-peptide transcriptional attenuators to create a hybrid RNA mechanism that uses sequential control of translation then transcription to achieve large dynamic range repression and activation (18). Importantly, this study showed that multiple RNA structures can be combined together to regulate several aspects of gene expression.

A notable feature of RNA regulatory mechanisms is that they regulate transcription, translation and mRNA degradation through the conditional formation of simple hairpin structures at defined positions in mRNAs (19). Specifically, intrinsic transcriptional terminators repress transcription by causing the dissolution of the transcription elongation complex (20,21), ribosome binding site (RBS)-sequestering hairpins block translation by inhibiting ribosome binding (22,23), and stability hairpins can prevent the activity of RNases to control mRNA degradation (24,25). The common connection between structure and function exhibited by RNA regulatory mechanisms reveals an intriguing possibility of engineering hairpin structures that can regulate multiple control points within a single mechanism.

We sought to use this approach on the pT181 attenuator from the *Staphylococcus aureus* plasmid pT181 (26), which has previously been shown to be useful for engineering a growing number of RNA networks (2,10,27). In its native form, the pT181 attenuator is encoded in the 5′ untranslated region of the plasmid replication protein RepC mRNA. Without the *cis*-encoded antisense RNA repressor, the sense RNA attenuator folds into a structure that allows for transcription of the RepC mRNA. When the antisense RNA is present, its binding to the sense RNA target permits the formation of an intrinsic transcriptional terminator upstream of the RepC coding sequence thereby terminating transcription (Figure 1).

A number of RNA engineering strategies have used the pT181 attenuator as a starting point to create RNA genetic networks and gene expression logics. Earlier studies concluded that the attenuator primarily regulates transcription (28), leading initial engineering efforts to use a transcriptional fusion of the attenuator to create basic RNA transcriptional repressors (2). This transcriptional fusion (28) included a fragment of the RepC coding sequence followed by a stop codon and a separate ribosome binding site for translation of the downstream gene of interest after the transcriptional decision was made by the attenuator (Figure 1A). This configuration initially exhibited only 64% repression, but was improved by strengthening the base of the terminator (20) through the addition of GC pairs to achieve 85% repression (2). Subsequent work used this system to build a library of independently acting, or orthogonal, transcriptional repressors that only repress their cognate targets with minimal cross talk with other variants (29). Orthogonal pairs of regulators are important for networks to function as expected by only controlling target genes as desired without interfering with off target expression. Recently, the pT181 mechanism was used to build RNA transcriptional activators (3), and a variety of genetic networks including logic gates (2,3), transcriptional cascades (2) and genetic networks that sequentially activate multiple genes (10).

Intriguingly, early studies on the natural pT181 attenuator mechanism hypothesized that an AGGAG sequence embedded in the 3′ half of the terminator hairpin was the ribosome binding site for *repC* (30). This would suggest that the terminator hairpin of the pT181 attenuator could also function by occluding the RBS to regulate translation as well as transcription. Later, it was determined that the pri-

mary mechanism of repression was transcription by comparing transcriptional versus translational reporter gene fusions (28). However, the presence of a near canonical RBS sequence in the 3′ terminator hairpin, spaced 12 nt from the start codon of *repC* suggests the possibility that the pT181 mechanism may in fact have a more powerful effect on gene expression by simultaneously regulating transcription and translation through the conditional formation of a single compact hairpin in response to interactions with an antisense RNA (Figure 1B).

In this work, we show that antisense-mediated repression of gene expression can be improved by utilizing the native RBS and thus the natural dual transcriptional/translational regulation of the pT181 attenuator. When configured as a translational fusion, we show we can increase the percent repression (100%-OFF gene expression level/ON gene expression level) of a fluorescent reporter protein from 85% (±3.4%) to 98% (±0.4%) in *Escherichia coli*. The success of this strategy led us to use it to improve the fold activation (ON gene expression level/OFF gene expression level) of a small transcription activating RNA (STAR) system based on the pT181 hairpin from 10-fold (±3.7) to 923-fold (±213). Our next goal was to create a library of orthogonal dual control repressors that can function independently in the same cell as components of larger genetic networks. To do this, we converted previously published orthogonal pT181 variants that functioned at the transcriptional level (29) into dual control regulators. Interestingly, this library of dual control repressors showed significant cross-talk, indicating that the dual control system breaks orthogonality, likely by increasing the opportunity for non-cognate antisense RNAs to bind and induce translational repression. To mitigate this, we engineered a minimal antisense RNA that reduced crosstalk thereby allowing the repressors to function independently. Finally, to demonstrate that these regulators can be used to fix leak within RNA genetic networks and that orthogonal versions can function in the same cell without breaking network function, we constructed a repressor cascade using the dual control repressor on the bottom level and found that the dual control cascade exhibited reduced network leak and had a higher dynamic range.

MATERIALS AND METHODS

Plasmid construction

Key sequences can be found in Supplementary Table S1. All the plasmids used in this study can be found in Supplementary Table S2 and plasmid diagrams in Supplementary Figure S1. The pT181 repressor and antisense plasmids, the pT181 mutant repressor and antisense plasmids, and the no-antisense control plasmid were constructs pAPA1272, pAPA1256, pAPA1273, pAPA1257 and pAPA1260, respectively, from Lucks *et al.* (2). The top level of the cascade was the theophylline pT181 mutant antisense plasmid, construct pAPA1306, from Qi *et al.* (31). The middle level of the cascade was modified from construct pAPA1347 from Lucks *et al.* (2) using Golden Gate assembly (32). The bottom level of the transcriptional cascade was construct pJBL1855 from Takahashi *et al.* (10) and the bottom level of the dual control cascade was modified from this construct using Golden Gate assembly. The antisense and repressor plasmids were constructed using inverse PCR (iPCR).

Strains, growth medium, and *in vivo* end point gene expression

All experiments were performed in *E. coli* strain TG1. Experiments were performed for at least seven biological replicates, (independent transformants of an isogenic strain unless otherwise noted) collected over three separate days. Plasmid combinations were transformed into chemically competent *E. coli* TG1 cells, plated on Difco LB + Agar plates containing 100 μg/ml carbenicillin and 34 μg/ml chloramphenicol and incubated overnight at 37°C. Plates were taken out of the incubator and left at room temperature for ∼9 h. Three colonies were picked and used to inoculate 300 μl of LB containing carbenicillin and chloramphenicol at the concentrations above in a 2 ml 96-well block (Costar 3960), and grown ∼17 h overnight at 37°C at 1000 rpm in a Labnet Vortemp 56 benchtop shaker. Six microliters of each overnight culture was then added to separate wells on a new block containing 294 μl (1:50 dilution) of supplemented M9 minimal media (1xM9 minimal salts, 1 mM thiamine hydrochloride, 0.4% glycerol, 0.2% casamino acids, 2 mM $MgSO_4$, 0.1 mM $CaCl_2$) containing the selective antibiotics and grown for 4 h at the same conditions as the overnight culture. Cultures (6–12 μl) were then transferred into a FACS round-bottom 96-well plate with 244 μl of PBS containing 2 mg/ml Kanamycin to stop translation. The plate was then read on a BD LSR II using the high throughput setting with the high throughput sampler (HTS). The samples for Figure 2C were transferred to Falcon 5 ml polystyrene round-bottom tubes and analyzed on a BD Aria Fusion. Growth information for glycerol stocks of an individual transformant for the cascade experiment is described in Supplementary Note S1.

Flow cytometry data collection

Data for the following parameters were collected on the BD LSR II: forward scatter (FSC), side scatter (SSC) and SFGFP (33) fluorescence (488 nm excitation, 515–545 nm emission). Three to 10 ul of each sample was measured in high throughput mode. Each sample was required to have at least 5000 counts, but most had 10 000–50 000. Counts were gated in FSC versus SSC by choosing a window surrounding the largest cluster of cells. SFGFP fluorescence values were recorded in relative channel number (1–262,144 corresponding to 18-bit data) and the geometric mean over the gated data was calculated for each sample. Data for Figure 2C was collected on a BD Aria Fusion for the following parameters: forward scatter (FSC), side scatter (SSC), SFGFP fluorescence (488 nm excitation, 530 nm emission), and mRFP Fluorescence (561 nm excitation, 582 nm emission). SFGFP and mRFP fluorescence values were recorded in relative channel number (1–262,144 corresponding to 18-bit data) and the geometric mean over the gated data was calculated for each sample. Compensation was calculated automatically by the BD Aria FACSDiva software using the compensation setup feature.

Flow cytometry data analysis

Data analysis and FACS calibration was performed according to the supplementary info of Lucks *et al.* (2). Spherotech 8-Peak Rainbow Calibration Beads (Spherotech cat. no. 559123) were used to obtain a calibration curve to convert fluorescence intensity (geometric mean, relative channel number) into MEFL units for SFGFP fluorescence or Molecules of Equivalent Phycoerythrin (MEPE) for RFP fluorescence. For each experiment, data for a set of control cultures was also collected which consisted of *E. coli* TG1 cells that do not produce SFGFP (transformed with control plasmids JBL001 and JBL002). The mean MEFL or MEPE value of TG1 cells without SFGFP or mRFP expression, respectively was subtracted from each colony's MEFL or MEPE value. Mean MEFL or MEPE values were calculated over replicates and error bars represent the standard deviation. For repressors, the OFF level is the MEFL or MEPE of cells containing the sense plasmid and the antisense plasmid and the ON level is the MEFL or MEPE of cells containing the sense plasmid and a no-antisense control plasmid. The percent repression for each antisense RNA/attenuator plasmid combination was calculated by subtracting the OFF level divided by the ON level from 1 (1 – OFF/ON). For activators the ON level is the MEFL or MEPE of cells containing the sense plasmid and the antisense plasmid and the OFF level is the MEFL or MEPE of cells containing the sense plasmid and a no-antisense control plasmid. The fold activation was calculated by dividing the ON level by the OFF level (ON/OFF).

In vivo bulk fluorescence time course experiments

Strain, transformation, and media were all the same as for end point experiments described above, except 25 ug/ml of kanamycin was used in addition to the other selective antibiotics because the cascade is encoded by three plasmids. Transformation plates containing *E. coli* TG1 cells transformed with three cascade plasmids (Supplementary Table S2) were taken out of the incubator and left at room temperature for ∼3 h. Three colonies were picked and used to inoculate 300 μl of LB containing selective antibiotics in a 2 ml 96-well block (Costar 3960), and grown ∼17 h overnight at the same conditions as described for an end point experiment. Twenty microliters of each overnight culture was then added to separate wells on a new block containing 980 μl (1:50 dilution) of supplemented M9 minimal media (as mentioned above) containing the selective antibiotics and grown for 4 h at the same conditions as the overnight culture. The optical density (OD, 600 nm) was then measured by transferring 50 μl of culture from the block into a 96-well plate (Costar 3631) containing 50 μl of phosphate buffered saline (PBS) and measuring using a Biotek Synergy H1m plate reader. The cultures were diluted into 1 ml of fresh M9 minimal media to an optical density of 0.015 and grown for 4 h. Then theophylline was added to the theophylline condition to a final concentration of 2 mM. Every 30 min for the next 4 h, 50 μl from each of the fresh cultures was removed from the 96-well block and transferred to a 96-well plate (Costar 3631) containing 50 μl of phosphate buffered saline (PBS). SFGFP fluorescence (FL, 485 nm excitation, 520 nm emission) and optical density (OD, 600 nm) were then measured at each time point using a Biotek Synergy H1m plate reader.

Bulk fluorescence data analysis

On each 96-well block, there were two sets of controls; a media blank (M9 alone) and *E. coli* TG1 cells that do not produce SFGFP (transformed with control plasmids JBL001, JBL002 and JBL1856). The block contained three replicates of each control. OD and FL values for each colony at each time point were first corrected by subtracting the corresponding values of the media blank at that same time point. The ratio of FL to OD (FL/OD) was then calculated for each well (grown from a single colony), and the mean FL/OD of TG1 cells without SFGFP at the same time point was subtracted from each colony's FL/OD value to correct for cellular autofluorescence. Experiments were performed for nine biological replicates collected over three separate days. One day is shown in Figure 6 while all three days are shown together in Supplementary Figure S2. Data for the experiment performed from glycerol stocks of an individual transformant is shown in Supplementary Figure S3 and data collection is described in Supplementary Note S1.

RESULTS

Regulating both transcription and translation with a single RNA structure improves dynamic range

We first sought to evaluate the performance of the dual control repressor by configuring it as a translational fusion with a downstream reporter gene (Figure 1B). Because the terminator hairpin contains a canonical RBS in its 3′ half, we would expect this configuration to regulate both transcription *and* translation of the downstream gene. Specifically, in the presence of antisense RNA, the formation of the terminator hairpin should both repress transcription of the downstream gene, as well as occlude the initiation of translation of any mRNA transcripts that were extended due to imperfect termination efficiency. Thus, we expected the dual control translational fusions to exhibit lower OFF levels than the transcription-only regulators.

In previous work, a translational fusion of the pT181 attenuator to the *lacZ* gene exhibited 62% repression in the presence of an antisense RNA as measured by Miller assays (28). Since the terminator of the pT181 system had been previously engineered (2) to strengthen the terminator stem base in order to increase transcriptional repression (20), we began by assessing the observed antisense-mediated repression of both the natural and engineered terminator using a translational fusion between *repC* and an SFGFP reporter gene (Figure 2A,B). To characterize attenuator function, plasmids were constructed such that each attenuator was placed downstream of a constitutive promoter and upstream of the SFGFP coding sequence on a medium copy plasmid. Complementary antisense RNAs were placed on a separate high copy plasmid downstream of the same constitutive promoter (Supplementary Table S1). Each attenuator plasmid was transformed into *E. coli* TG1 cells along with either its cognate antisense or a no-antisense control plasmid (Supplementary Table S2). Individual colonies were picked, grown overnight, sub-cultured into minimal media

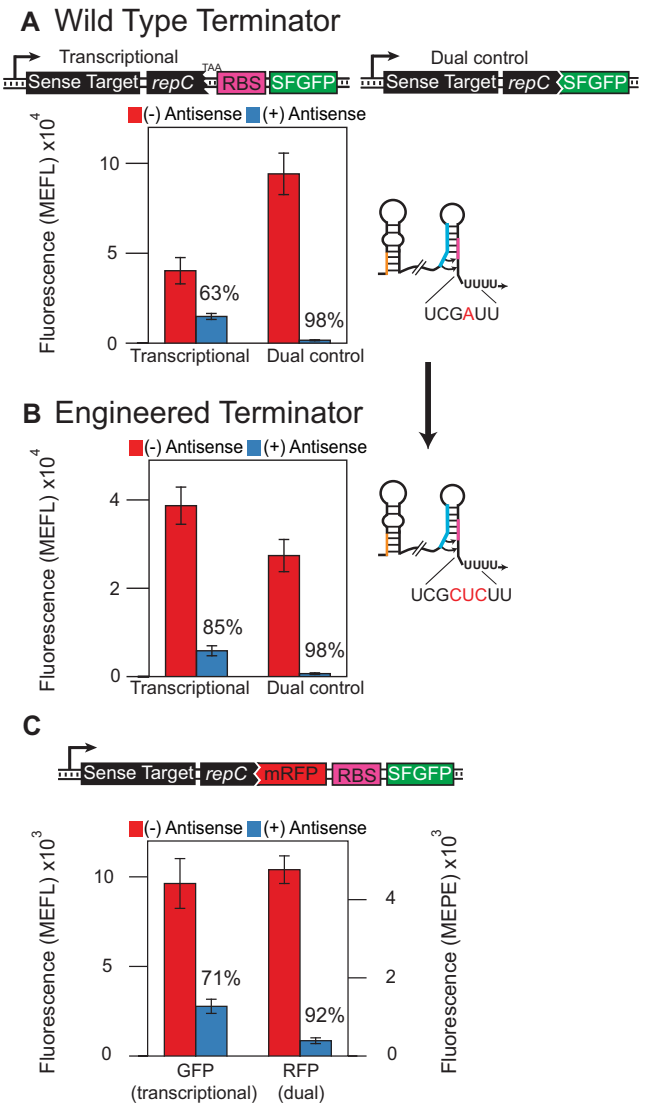

Figure 2. Dual transcription/translation control represses gene expression with higher dynamic range than transcription control *in vivo*. Functional characterization of the (**A**) wild type (28), or (**B**) engineered (2) attenuator configured to repress either transcription (transcriptional fusion) or dual transcription/translation (translational fusion) of an SFGFP coding sequence. Average fluorescence was collected by flow cytometry as Molecules of Equivalent Fluorescein (MEFL) of *E. coli* TG1 cells transformed with a plasmid expressing the indicated attenuator-SFGFP construct and a plasmid expressing the antisense RNA (+, blue) or a control plasmid lacking the antisense sequence (–, red) (Supplementary Table S2). Percent repression is labelled above each construct tested. In both cases the dual control regulator showed 98% repression (50-fold), though with a higher ON expression level for the wild type attenuator. Error bars represent standard deviations of at least seven biological replicates. Cartoons highlight differences between the wild type and engineered attenuator sequences, which differ by several bases in the 3′ half of the terminator hairpins (Supplementary Figure S8). (**C**) Testing dual control versus transcriptional control in a two-color operon construct. The wild type attenuator sequence was translationally fused to an mRFP coding sequence, which was followed by an RBS-SFGFP sequence. In this way, mRFP was under dual transcription/translation control while SFGFP was under only transcription control. The construct was tested as in (A) with mRFP fluorescence collected by flow cytometry as Molecules of Equivalent Phycoerythrin (MEPE). RFP was more strongly repressed at 92% (±1.7%) than GFP at 71% (±5.8%). Averages and standard deviations plotted in (A) and (B) are presented Supplementary Table S3 to allow for comparison within orders of magnitude.

and grown until logarithmic growth was reached. Fluorescence was measured for each culture using flow cytometry (see materials and methods). Using this experimental design, we observed a 63% (±7.9%) repression in gene expression for the wild-type transcriptional fusion that increased to 98% (±0.4%) when a translational fusion was used (Figure 2A). A closer examination of the increase in repression revealed that the translational fusion not only decreased the OFF level of gene expression in the presence of antisense, but also increased the ON level in the absence of antisense.

We performed the same fluorescence experiment described above with the engineered terminator and found an improvement from 85% (±3.4%) repression to 98% (±0.7%) repression (Figure 2B). However, in this case the ON level was reduced for the translational fusion, which could be due to the terminator mutation causing increased spacing between the RBS and the start codon of *repC*. This suggested that the *repC* context of the dual control system could be important. To test this, we fully removed the *repC* sequence and characterized the dual control attenuator. We found that when *repC* is fully removed, the ON level is reduced (Supplementary Figure S4), possibly due to the sequence context change. For this reason, we chose to continue with the wild type translational fusion repressor including a 12nt fusion of *repC*.

To further investigate the mechanism of the attenuator, we performed qRT-PCR experiments on a transcriptional and a translational fusion construct (Supplementary Figure S5). The transcriptional attenuator with the engineered terminator showed 80% (±3.4%) repression when measuring SFGFP fluorescence and 78% (±9.1%) repression when measuring SFGFP transcripts with qRT-PCR, indicating that repression comes primarily from transcriptional termination. The dual control attenuator with the wild-type terminator showed 97% (±0.7%) repression when measuring SFGFP fluorescence and 84% (±8.1%) repression when measuring SFGFP transcripts with qRT-PCR, indicating that the increased repression is due to the added translational control.

We next designed a construct to compare dual transcription/translation control to transcription-only control using a dual reporter protein operon (Figure 2C). In this design, mRFP is translationally fused to the attenuator, while SFGFP is translated from an independent downstream RBS. In this way, we would expect mRFP to be regulated at both the transcriptional and translational levels, while SFGFP would be regulated at just the transcriptional level leading to overall increased repression for mRFP. We transformed cells with the sense target plasmid and the antisense repressor or a blank control plasmid and measured the fluorescence using flow cytometry. As expected, we found that mRFP was repressed more effectively (92% +/- 1.7%) than SFGFP (71 ± 5.8%). This result also demonstrated that the dual control repressor can be modularly used to regulate different proteins as well as operons.

The dual control strategy can be extended to a pT181-based activator to dramatically improve fold activation

We next sought to determine if the dual control strategy could be applied to an RNA-based transcriptional activator mechanism derived from the pT181 system. Small transcription activating RNAs (STARs) were recently engineered to activate, rather than repress, transcription in the presence of designed antisense RNAs (3). In the STAR mechanism, the sense target region consists of a transcriptional terminator placed upstream of a target gene which blocks transcription elongation to form the OFF state in the absence of a STAR antisense RNA (Supplementary Figure S6). The addition of a STAR antisense RNA, designed to contain an anti-terminator sequence complementary to the 5′ half of the terminator stem, prevents terminator formation, allowing transcription to proceed and gene expression to be ON. Early investigations showed that the pT181 attenuation system could be converted into a STAR by using the terminator sequence from pT181 and an appropriately designed STAR antisense RNA (3). This gave us the opportunity to examine whether a dual control strategy would be effective in the context of gene expression activation.

We constructed a dual control activator by making a translational fusion using one of the pT181 STARs (Supplementary Table S1) (Figure 3A). To characterize dual control and transcription-only STAR activator function, each sense target plasmid was transformed into *E. coli* TG1 cells along with either its cognate STAR antisense or a no-antisense control plasmid (Supplementary Table S2). Individual colonies were picked, grown overnight, sub-cultured into minimal media and grown until logarithmic growth was reached. Fluorescence was measured for each culture using flow cytometry (see Materials and Methods). The dual control strategy improved transcription-only activation from 10-fold (±3.7) to 923-fold (±213) respectively, due to both a higher ON level and a lower OFF level. Notably the OFF level for the dual-control STAR system was remarkably close to the background cellular autofluorescence level (Figure 3C).

Multiple dual control regulators can be built using pT181 mutants and chimeras

We next sought to determine if the dual control strategy could be applied to additional transcriptional attenuators to improve their dynamic range. Multiple orthogonal, or independently acting, pairs of antisense/attenuators are needed in order to build more sophisticated genetic networks. Since a library of orthogonal pT181 transcriptional regulators has previously been engineered (29), we first sought to apply the dual control strategy to these additional regulators. To create orthogonal antisense/attenuator pairs, the library includes several pT181 specificity changing mutants in the first attenuator hairpin that affect antisense recognition, as well as chimeric fusions of the pT181 mechanism with RNA kissing-hairpin interaction regions taken from translational repressors. However, in order to preserve their overall function, the pT181 mutants and fusions are very similar in sequence, including the pT181 terminator hairpin, allowing us to make translational fusions to test the dual control strategy in these mutant contexts.

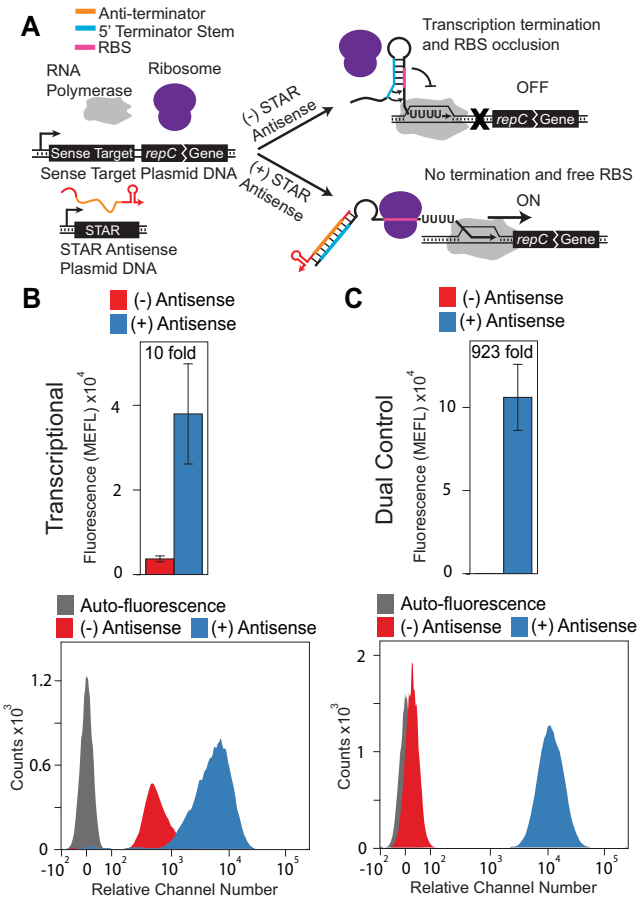

Figure 3. Converting a small transcription activating RNA (STAR) mechanism to a dual transcription/translation activator enhances fold activation. (**A**) Schematic of the proposed dual transcription/translation activation mechanism. The sense target region consists of the pT181 STAR target region from Chappell *et al.* (3) followed by 12 nt of the *repC* gene translationally fused to SFGFP. In the absence of the STAR RNA (red/orange), the terminator forms, preventing downstream transcription by RNA polymerase (gray). This structure also occludes the RBS inside the 3′ side of the terminator hairpin, which prevents ribosome binding. Thus, in the absence of STAR RNA, the mechanism is transcriptionally and translationally OFF. The STAR RNA contains an anti-terminator sequence (orange) complementary to the 5′ half of the terminator (blue). When present, the STAR RNA binds to the terminator, preventing terminator formation and allowing transcription elongation. This structure also exposes the RBS, allowing ribosome binding and translation. Thus, in the presence of STAR RNA, the mechanism is transcriptionally and translationally ON. The original transcriptional mechanism is shown in Supplementary Figure S6. Sequences and structures are shown in Supplementary Figure S11. (**B**) Functional characterization of a pT181 STAR that controls transcription. Average fluorescence (MEFL) (top) was collected by flow cytometry of *E. coli* TG1 cells transformed with a plasmid expressing the STAR target transcriptionally fused to an SFGFP coding sequence and a plasmid expressing the STAR RNA (+, blue) or a control plasmid lacking the STAR sequence (–, red) (Supplementary Table S2). Error bars represent standard deviations of at least seven biological replicates. The flow cytometry histogram data (bottom) is plotted on a bi-exponential graph (38). Auto-fluorescence indicates the observed fluorescence distribution from *E. coli* TG1 cells transformed with plasmids lacking STAR target-SFGFP fusion or antisense cassette (Supplementary Table S2). (**C**) Functional characterization of a pT181 STAR that controls both transcription and translation. Data was collected and plotted as in (B). The dual control strategy increases fold activation from 10-fold (±3.7) to 923 fold (±213) by increasing the ON expression as well as decreasing the OFF expression to near-background auto-fluorescence levels. Averages and standard deviations plotted in (B) and (C) are presented Supplementary Table S4 to allow for comparison within orders of magnitude.

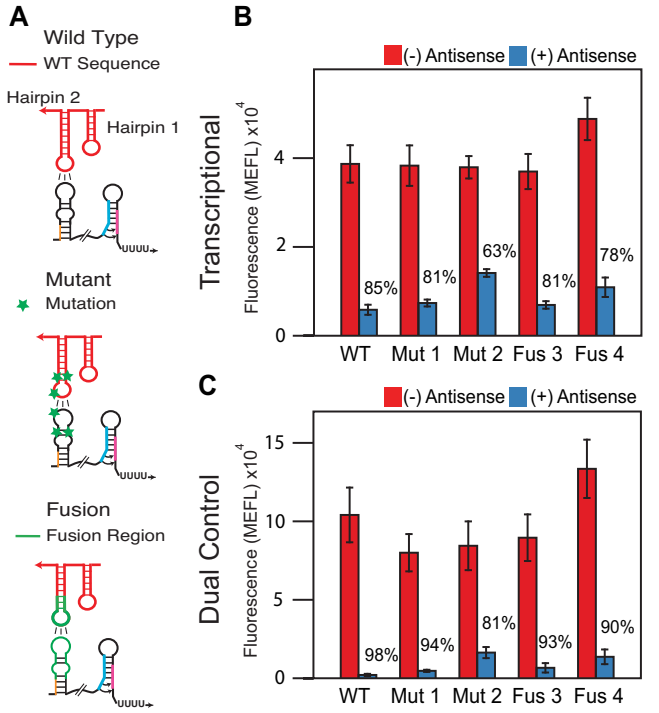

Figure 4. The dual transcription/translation control strategy functions across orthogonal pT181 mutants and chimeras. (**A**) Schematics of the interactions between the dual control sense target region and the corresponding cognate antisense RNA for wild type, specificity mutants and chimeric fusions engineered to change the specificity of the antisense–attenuator interactions. Sequences and structures are shown in Supplementary Figure S12. (**B**) Functional characterization of the transcriptional wild type pT181 repressor (WT), two mutants (Mut 1,2) (2) and two chimeric fusions (Fus 3,4) (29). Each repressor contained the wild type terminator region depicted in Figure 2A. Functional characterization and data presentation as in Figure 2. Error bars represent standard deviations of at least seven biological replicates. (**C**) As in (B) except with each repressor configured as a dual transcription/translation controller. Using the dual control strategy improves the repression of the transcriptional attenuators. Averages and standard deviations plotted in (B) and (C) are presented in Supplementary Table S5 to allow for comparison within orders of magnitude.

Additional dual control repressors were characterized as above and compared to the repression observed in the transcription-only regulatory configuration. Specifically, we tested the transcriptional wild type (WT) repressor, the mutant repressors (Mut 1,2) (2) and fusion repressors (Fus 3,4) (29) and observed between 63% and 85% repression (Figure 4B). We then tested the dual control repressors made from the same attenuators and found that repression increased to between 81% and 98% (Figure 4C) averaging to a 15% increase in repression with the wild type pT181 remaining the best dual control repressor. As before, these increases in dynamic range come from both a higher ON level and a lower OFF level (Figure 4).

Orthogonal dual control repressors can be engineered by reducing the antisense RNA sequence

We next sought to test the orthogonality of the dual control repressors. In addition to requiring multiple dual control regulators to build genetic networks, these regulators must also be orthogonal, or only interact with their cognate target. Previous work showed that the original transcription-only chimeric fusions exhibited limited crosstalk between non-cognate antisense/sense target pairs, making them highly orthogonal (29). To test this for our dual control repressors, we challenged each repressor sense target with all non-cognate antisense RNAs to form an orthogonality matrix (Figure 5B, Supplementary Figure S7A).

Despite starting from a set of highly orthogonal transcriptional repressors, we observed significant crosstalk between the dual control regulators. Earlier work on elucidating the mechanism of antisense-mediated translation repression suggested that flanking sequences in the antisense RNA can form extended interactions with the sense target RNAs (34). We thus hypothesized that portions of the antisense RNAs can be interacting with the sense target to repress translation even after the transcriptional regulatory decision has been made. To test this hypothesis, we truncated the antisense RNA sequence to the elements necessary for initial RNA-RNA kissing-hairpin interactions that were shown to be essential for the transcriptional regulatory decision (11). Specifically, hairpin 2 of the pT181 antisense makes contact with the first hairpin of the sense target region of the attenuator that contains the anti-terminator (Supplementary Figure S8). We hypothesized that we could remove the antisense hairpin 1 and truncate the end of hairpin 2 to reduce cross-talk between the dual control repressors (Figure 5A, Supplementary Figure S9). Using these reduced antisense RNAs, we repeated the orthogonality matrix and observed that crosstalk was reduced for most non-cognate interactions (Figure 5C, Supplementary Figure S7B). However, not all crosstalk was reduced. Notably sense/antisense pairs that began with low crosstalk values, displayed increased crosstalk using the truncated antisense. For example the pair consisting of fusion 4 antisense targeting the fusion 3 sense target rose significantly from 7% to 27% to become the highest crosstalk. However, generally those non-cognate pairs that started at higher crosstalk were more significantly reduced (reduced 21% on average for those above 20% crosstalk) compared to those that started at lower crosstalk (raised 0.5% on average for those below 20% crosstalk).

The dual control repressor mitigates network leak in an RNA repressor cascade

Finally we sought to test the dual control regulators in an RNA-only network context that would demonstrate how reduced leak improves network performance and confirm that orthogonal versions can function correctly in the same cell. RNA repressor cascades were the first RNA-only network built (2) and have been used to highlight the fast speed of RNA genetic networks (10). The repressor cascade also acts as a modular unit that can be built upon to create more sophisticated networks such as one that controls the timing of a sequence of genes in response to a single input (10,35). However, past attempts at characterizing repressor cascades have revealed that the network leaks due to insufficient repression of the individual regulators resulting in un-desired gene expression in conditions where the overall network is designed to be OFF. We therefore sought to fix the leak of an RNA repressor cascade using the dual control repressor. To

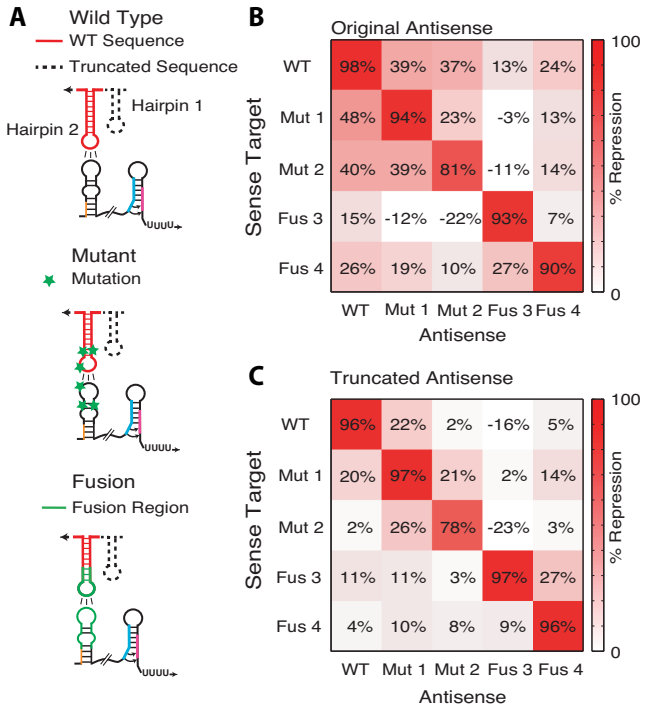

Figure 5. Truncated antisense RNA improves orthogonality between dual transcription/translation RNA repressors. (**A**) Schematics of the interactions between the dual control sense target region and the corresponding cognate antisense RNA for wild type, specificity mutants and chimeric fusions. Dashed lines show portions of the antisense RNA structure that were truncated to reduce cross talk between pairs of dual transcription/translation control RNA repressors and targets. Hairpin 1 and unnecessary regions (4 nt) at the 3′ end of the antisense were deleted. Sequences and structures for the wild type pT181 antisense are show in Supplementary Figure S9. (**B**) An orthgonality matrix showing percent repression observed when sense targets were co-expressed with different full-length antisense RNAs. Each element of the matrix represents the percent repression observed from the indicated antisense/sense target plasmid combination compared to a no-antisense/sense target plasmid condition using functional characterization experiments as in Figure 2. (**C**) As in (B) with truncated forms of the antisense RNAs depicted in (A), showing reduction in repression when non-cognate truncated antisense is present (off diagonal elements). Barplots depicting the data in (B) and (C) are shown in Supplementary Figure S7. Standard deviations for the data in (B) and (C) are shown in Supplementary Tables S6 and S7.

test this, we built an RNA repressor cascade that activates the expression of SFGFP in response to theophylline (Figure 6A). Theophylline was chosen because a theophylline activated antisense allows us to build an RNA-only network that can directly respond to this small molecule (31). However, we also verified that other inducible promoter systems can be used to induce antisense expression and tune repression (Supplementary Figure S10). The cascade consists of three plasmids each expressing one level of the network. Without theophylline present, antisense repressor RNA 2 represses sense target RNA 2 and SFGFP expression. When theophylline is added, it activates antisense repressor RNA 1, which is normally non-functional in the absence of theophylline due to a designed interaction between the antisense RNA hairpin and a fused theophylline aptamer (31). In this way, theophylline binding allows antisense repressor RNA 1 to repress antisense repressor RNA 2, allowing SGFP to be expressed. Overall, when theophylline is added to the cell culture, an RNA signal induces SFGFP expression.

To compare RNA cascades that use either transcription-only or dual control SGFP expression, we performed time course experiments on *E. coli* cultures that contained the cascade plasmids with either the transcriptional or dual control repressor cascade plasmids for the bottom level of the cascade. After incubating overnight in LB media, the cultures were diluted into M9 supplemented media and incubated for four hours. The cultures were then diluted again into fresh M9 media to a consistent OD and incubated for four more hours. From here, we sampled cultures every 30 min to measure SFGFP fluorescence and culture OD over time. Theophylline was added to some cell cultures at the beginning of sampling to measure the cascade response (Figure 6B). This experiment was repeated on three separate days, with the first day shown in Figure 5B and the other two shown in Supplementary Figure S2. In addition we performed a version of this experiment from glycerol stocks which showed similar results (Supplementary Figure S3). As expected, when theophylline was introduced to both the transcriptional and dual control cascades, we observed SFGFP activation that continued throughout the rest of the time course. However, the transcriptional version of the network displayed significant leak (Figure 6B, green curves) in comparison to the dual control network, which displayed a lower baseline expression (Figure 6B, blue curves) and thus a greater dynamic range. The leak in the transcriptional version of the network is a direct result of the leaky transcriptional repressor—even when in the OFF state, terminator read through can lead to translation of downstream transcripts since their RBS is not masked within a secondary structure. In the dual control case however, the masking of the RBS within the terminator structure prevents this aberrant translation leading to reduced OFF states throughout. This result demonstrated that dual control repressors can not only be used in an RNA genetic network, but that their use reduced overall leak through the network to improve its desired function.

DISCUSSION

In this work, we have demonstrated the utility of an RNA structure that regulates both transcription and translation in a single, compact mechanism by showing that it improves dynamic range of antisense RNA-mediated control of gene expression and reduces leak when used in RNA genetic networks. Specifically, translational fusions between the pT181 attenuator and downstream reporter genes allowed the transcription of these genes to be regulated by the pT181 terminator hairpin and the translation of these genes by the *repC* RBS sequence encoded in the 3′ half of the same hairpin. In this way, the formation of the OFF structure in the presence of a cognate antisense RNA allows gene expression to be repressed at two levels, and thereby improves repression from 85% (±3.4%) for the transcriptional-only case to 98% (±0.4%) in the dual control case. In addition to decreasing OFF levels in the presence of antisense RNA, this configuration increased the ON level in the absence of antisense RNA.

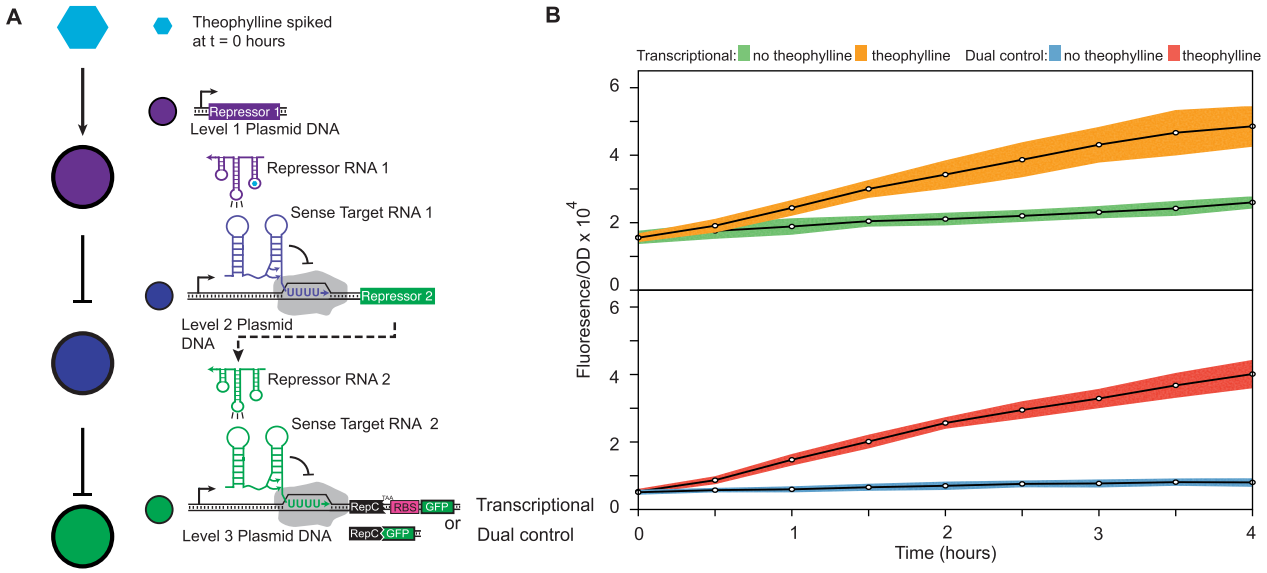

Figure 6. The dual transcription/translation control strategy mitigates leak in an RNA repressor cascade. (**A**) Schematic of the theophylline activated RNA repressor cascade. The level three SFGFP gene expression is controlled by sense target region 2, which is repressed by repressor RNA 2. Repressor RNA 2 is in turn controlled by the upstream sense target region 1, which is repressed by repressor RNA 1. Repressor RNA 1 is a fusion with a theophylline aptamer (31) that is active only with theophylline bound. Without theophylline, repressor RNA 1 is inactive causing overall repression of SFGFP (OFF). When theophylline is added to the cell culture media, the repressor RNA 1 represses transcription of repressor RNA 2, leading to SFGFP expression (ON). The level three attenuator was configured to regulate SFGFP either transcriptionally, or using the dual transcription/translational control mechanism. (**B**) Functional time course characterization of the transcriptional and dual control repressor cascades. Three plasmids each encoding one of the network levels were co-transformed into *E. coli* TG1 cells, grown overnight and sub-cultured into fresh M9 minimal media for 4 h before starting the time-course with a fresh sub-culture (see Materials and Methods). After 4 h of growth in M9, theophylline (2 mM) was added to the media causing SFGFP to be expressed (orange for transcriptional and red for dual control). Time points were sampled every 30 min for 4 h. Bulk fluorescence and OD600 were measured using a plate reader. The no theophylline condition is shown in green for the transcriptional cascade and blue for dual control. The dual control regulator reduces the overall background fluorescent level while maintaining a similar ON level and thus improves dynamic range. The data shown here are from three individual transformants on a single day. Data for the three independent experiments performed on separate days are shown together in Supplementary Figure S2. The colored region indicates the standard deviation from three biological replicates.

To further investigate the mechanistic details of the dual control repressors we performed qRT-PCR experiments (Supplementary Figure S5). The transcriptional attenuator displayed similar SFGFP fluorescence repression (80%) and SFGFP transcript repression (78%) measured by qRT-PCR, while the dual control attenuator revealed improved SFGFP fluorescence repression (97%) over SFGFP transcript repression (84%). This indicates that some of the improvement is due to the added translational control. The dual control improvement in repression comes from both an increased ON level in the absence of antisense RNA and a decreased OFF level when antisense is present as compared to the transcriptional attenuator. The increased ON level could be due to increased RBS exposure due to RNA structural context around the RBS and the start codon with the RNA is in the anti-terminated structure (Supplementary Figure S8). A similar structural effect has recently been seen in the *B. cereus crcB* fluoride riboswitch in which the anti-terminated form shows increased RBS exposure (36). In addition, the translational fusion allowed an optimal distance between the RBS and the start codon (Supplementary Figure S8) allowing for more efficient access to the ribosome and greater frequency of translation initiation. We also observed a reduction in the mRNA OFF level in the dual control scenario as compared to the transcriptional attenuator when measuring SFGFP transcripts using qRT-PCR. This effect could be a result of a decrease in translation in the tightly regulated OFF state, which could reduce ribosome protection of the mRNA to allow more efficient mRNA degradation.

Interestingly, our results are different from those observed by previous studies of the pT181 attenuator (28). Through comparing transcriptional vs. translational fusions of the pT181 attenuator to the LacZ reporter gene, this study observed 62% repression for the translational fusion and 50% for the transcriptional fusion. The lack of significantly different results and the presence of an intrinsic terminator sequence indicated that the attenuator functioned primarily through transcriptional repression. It is possible that our system shows a more significant difference because of the increased sensitivity afforded by our use of SFGFP expression. Nevertheless, our findings strongly suggest that the natural pT181 attenuator system likely regulates at both the transcriptional and translational levels.

Overall the dual control mechanism significantly improved the dynamic range of RNA regulators over RNA transcriptional repressors and is better than the ∼90% repression seen for the best RNA translational repressors (14) and the 85% repression seen for the best transcriptional RNA repressors (2). In addition to the pT181 dual control repressor, we also engineered a pT181 STAR activator and increased its activation in response to STAR antisense RNA from 10-fold (±3.7) to 923 fold (±213). This improves upon the previously published fold activation of

transcriptional STAR regulators (90-fold (3)) and translational toehold regulators (∼400-fold (5)). We also showed that this strategy could be expanded to additional pT181 mutant and fusion repressors, increasing the repression of several orthogonal regulators with this unique combination of transcriptional and translation control. Overall this is a significant increase in the number and capability of regulatory tools available for constructing genetic networks with tighter control, which is particularly useful for situations in which an RNA part with reduced leak is desired.

In order to build robust genetic networks in which the parts act independently and predictably the parts must be orthogonal or act independently of other regulators in the system. However, the initial dual control riboregulators exhibited significant crosstalk. We hypothesized that this was due to additional interactions between the antisense RNAs and the sense target RNAs that caused translation to be repressed even after the transcriptional decision had been made. For a transcriptional decision to be made, the antisense RNAs must interact cotranscriptionally. However, the antisense can still bind the dual control sense target after transcription and affect RBS availability. This would indicate that the modifications between mutants, fusions, and the original pT181 are enough to inhibit crosstalk during transcription but the increased time for antisense-sense target interactions before translation initiation allows shared sequences in non-cognate pairs more opportunity to interact. We therefore decided to reduce the redundant pT181 sequence to reduce the affinity of non-cognate antisense RNAs for sense target regions. While not all non-cognate antisense and sense target pairs were improved by the truncations, on average the worst performing pairs improved by 20% repression. By truncating redundant pT181 sequence we greatly improved orthogonality, making it possible to use these dual control repressors in RNA networks.

Finally, we used dual control RNA repressors to address a current problem with RNA only networks, which is leak that results from parts that do not allow complete repression of their targets. Specifically, we used the dual control repressor in a repressor cascade and found that it reduced network leak and background fluorescence. Additionally, the repressor cascade demonstrates that the orthogonal attenuators can function together in the same cell.

This work demonstrates a novel RNA motif that regulates multiple aspects of gene expression in a single compact mechanism, and that displays a dynamic range of gene regulation comparable to protein-based mechanisms. As such, this is another example of how RNAs may be optimized to function as well as proteins. We anticipate that as synthetic biology moves beyond the creation of regulator parts libraries and into building more sophisticated networks, RNA regulatory mechanisms such as dual control repressors will find increased use in designing RNA genetic networks with predictable function.

SUPPLEMENTARY DATA

Supplementary Data are available at NAR Online.

ACKNOWLEDGEMENTS

We acknowledge Cameron Glasscock (Julius Lucks Laboratory, Cornell University) for his help in reviewing and checking data processing, Eric Strobel (Julius Lucks Laboratory, Northwestern University) for insightful discussions of the pT181 mechanism and Sarai Meyer (Julius Lucks Laboratory, Cornell University) for her aid in the revision process in addition to reviewing and checking data processing.

FUNDING

Office of Naval Research Young Investigators Program Award (ONR YIP) [N00014-13-1–0531 to J.B.L.]; NSF CAREER Award [1452441 to J.B.L]; Searle Funds at The Chicago Community Trust [to J.B.L]. The open access publication charge for this paper has been waived by Oxford University Press - *NAR* Editorial Board members are entitled to one free paper per year in recognition of their work on behalf of the journal.
Conflict of interest statement. None declared.

REFERENCES

1. Strobel,E.J., Watters,K.E., Loughrey,D. and Lucks,J.B. (2016) RNA systems biology: uniting functional discoveries and structural tools to understand global roles of RNAs. *Curr. Opin. Biotechnol.*, **39**, 182–191.
2. Lucks,J.B., Qi,L., Mutalik,V.K., Wang,D. and Arkin,A.P. (2011) Versatile RNA-sensing transcriptional regulators for engineering genetic networks. *Proc. Natl. Acad. Sci. U.S.A.*, **108**, 8617–8622.
3. Chappell,J., Takahashi,M.K. and Lucks,J.B. (2015) Creating small transcription activating RNAs. *Nat. Chem. Biol.*, **11**, 214–220.
4. Qi,L.S., Larson,M.H., Gilbert,L.A., Doudna,J.A., Weissman,J.S., Arkin,A.P. and Lim,W.A. (2013) Repurposing CRISPR as an RNA-guided platform for sequence-specific control of gene expression. *Cell*, **152**, 1173–1183.
5. Green,A.A., Silver,P.A., Collins,J.J. and Yin,P. (2014) Toehold switches: de-novo-designed regulators of gene expression. *Cell*, **159**, 925–939.
6. Pardee,K., Green,A.A., Takahashi,M.K., Braff,D., Lambert,G., Lee,J.W., Ferrante,T., Ma,D., Donghia,N., Fan,M. *et al.* (2016) Rapid, low-cost detection of zika virus using programmable biomolecular components. *Cell*, **165**, 1255–1266.
7. Carrier,T.A. and Keasling,J.D. (1999) Library of synthetic 5′ secondary structures to manipulate mRNA stability in Escherichia coli. *Biotechnol. Prog.*, **15**, 58–64.
8. Carothers,J.M., Goler,J.A., Juminaga,D. and Keasling,J.D. (2011) Model-driven engineering of RNA devices to quantitatively program gene expression. *Science*, **334**, 1716–1719.
9. Pfleger,B.F., Pitera,D.J., Smolke,C.D. and Keasling,J.D. (2006) Combinatorial engineering of intergenic regions in operons tunes expression of multiple genes. *Nat. Biotechnol.*, **24**, 1027–1032.
10. Takahashi,M.K., Chappell,J., Hayes,C.A., Sun,Z.Z., Kim,J., Singhal,V., Spring,K.J., Al-Khabouri,S., Fall,C.P., Noireaux,V. *et al.* (2015) Rapidly characterizing the fast dynamics of RNA genetic circuitry with cell-free transcription-translation (TX-TL) systems. *ACS Synth. Biol*, **4**, 503–515.
11. Takahashi,M.K., Watters,K.E., Gasper,P.M., Abbott,T.R., Carlson,P.D., Chen,A.A. and Lucks,J.B. (2016) Using in-cell SHAPE-Seq and simulations to probe structure-function design principles of RNA transcriptional regulators. *RNA*, **22**, 920–933.
12. Zadeh,J.N., Steenberg,C.D., Bois,J.S., Wolfe,B.R., Pierce,M.B., Khan,A.R., Dirks,R.M. and Pierce,N.A. (2011) NUPACK: analysis and design of nucleic acid systems. *J. Comput. Chem.*, **32**, 170–173.
13. Lapique,N. and Benenson,Y. (2014) Digital switching in a biosensor circuit via programmable timing of gene availability. *Nat. Chem. Biol.*, **10**, 1020–1027.

14. Mutalik,V.K., Qi,L., Guimaraes,J.C., Lucks,J.B. and Arkin,A.P. (2012) Rationally designed families of orthogonal RNA regulators of translation. *Nat. Chem. Biol.*, **8**, 447–454.
15. Lee,Y.J., Hoynes-O'Connor,A., Leong,M.C. and Moon,T.S. (2016) Programmable control of bacterial gene expression with the combined CRISPR and antisense RNA system. *Nucleic Acids Res.*, **44**, 2462–2473.
16. Morra,R., Shankar,J., Robinson,C.J., Halliwell,S., Butler,L., Upton,M., Hay,S., Micklefield,J. and Dixon,N. (2016) Dual transcriptional-translational cascade permits cellular level tuneable expression control. *Nucleic Acids Res.*, **44**, e21.
17. Horbal,L. and Luzhetskyy,A. (2016) Dual control system – a novel scaffolding architecture of an inducible regulatory device for the precise regulation of gene expression. *Metab. Eng.*, **37**, 11–23.
18. Liu,C.C., Qi,L., Lucks,J.B., Segall-Shapiro,T.H., Wang,D., Mutalik,V.K. and Arkin,A.P. (2012) An adaptor from translational to transcriptional control enables predictable assembly of complex regulation. *Nat. Methods*, **9**, 1088–1094.
19. Chappell,J., Watters,K.E., Takahashi,M.K. and Lucks,J.B. (2015) A renaissance in RNA synthetic biology: new mechanisms, applications and tools for the future. *Curr. Opin. Chem. Biol.*, **28**, 47–56.
20. Ray-Soni,A., Bellecourt,M.J. and Landick,R. (2016) Mechanisms of bacterial transcription termination: all good things must end. *Annu. Rev. Biochem.*, **85**, 319–347.
21. Chen,Y.-J., Liu,P., Nielsen,A.A.K., Brophy,J.A.N., Clancy,K., Peterson,T. and Voigt,C.A. (2013) Characterization of 582 natural and synthetic terminators and quantification of their design constraints. *Nat. Methods*, **10**, 659–664.
22. Brantl,S. (2007) Regulatory mechanisms employed by cis-encoded antisense RNAs. *Curr. Opin. Microbiol.*, **10**, 102–109.
23. Espah Borujeni,A., Channarasappa,A.S. and Salis,H.M. (2014) Translation rate is controlled by coupled trade-offs between site accessibility, selective RNA unfolding and sliding at upstream standby sites. *Nucleic Acids Res.*, **42**, 2646–2659.
24. Carrier,T.A. and Keasling,J.D. (1997) Controlling messenger RNA stability in bacteria: strategies for engineering gene expression. *Biotechnol. Prog.*, **13**, 699–708.
25. Alifano,P., Bruni,C.B. and Carlomagno,M.S. (1994) Control of mRNA processing and decay in prokaryotes. *Genetica*, **94**, 157–172.
26. Novick,R.P., Iordanescu,S., Projan,S.J., Kornblum,J. and Edelman,I. (1989) pT181 plasmid replication is regulated by a countertranscript-driven transcriptional attenuator. *Cell*, **59**, 395–404.
27. Hu,C.Y., Varner,J.D. and Lucks,J.B. (2015) Generating effective models and parameters for RNA genetic circuits. *ACS Synth. Biol.*, **4**, 914–926.
28. Brantl,S. and Wagner,E.G.H. (2002) An antisense RNA-mediated transcriptional attenuation mechanism functions in Escherichia coli. *J. Bacteriol.*, **184**, 2740–2747.
29. Takahashi,M.K. and Lucks,J.B. (2013) A modular strategy for engineering orthogonal chimeric RNA transcription regulators. *Nucleic Acids Res.*, **41**, 7577–7588.
30. Kumar,C.C. and Novick,R.P. (1985) Plasmid pT181 replication is regulated by two countertranscripts. *Proc. Natl. Acad. Sci. U.S.A.*, **82**, 638–642.
31. Qi,L., Lucks,J.B., Liu,C.C., Mutalik,V.K. and Arkin,A.P. (2012) Engineering naturally occurring trans-acting non-coding RNAs to sense molecular signals. *Nucleic Acids Res.*, **40**, 5775–5786.
32. Engler,C., Kandzia,R. and Marillonnet,S. (2008) A one pot, one step, precision cloning method with high throughput capability. *PLoS ONE*, **3**, e3647.
33. Pédelacq,J.-D., Cabantous,S., Tran,T., Terwilliger,T.C. and Waldo,G.S. (2006) Engineering and characterization of a superfolder green fluorescent protein. *Nat. Biotechnol.*, **24**, 79–88.
34. Kolb,F.A., Engdahl,H.M., Slagter-Jäger,J.G., Ehresmann,B., Ehresmann,C., Westhof,E., Wagner,E.G. and Romby,P. (2000) Progression of a loop-loop complex to a four-way junction is crucial for the activity of a regulatory antisense RNA. *EMBO J.*, **19**, 5905–5915.
35. Alon,U. (2007) Network motifs: theory and experimental approaches. *Nat. Rev. Genet.*, **8**, 450–461.
36. Watters,K.E., Strobel,E.J., Yu,A.M, Lis,J.T. and Lucks,J.B. (2016) Cotranscriptional folding of a riboswitch at nucleotide resolution. *Nat. Struct. Mol. Biol.*, **23**, 1124–1131.
37. Brantl,S. and Wagner,E.G. (2000) Antisense RNA-mediated transcriptional attenuation: an in vitro study of plasmid pT181. *Mol. Microbiol.*, **35**, 1469–1482.
38. Parks,D.R., Roederer,M. and Moore,W.A. (2006) A new 'Logicle' display method avoids deceptive effects of logarithmic scaling for low signals and compensated data. *Cytometry A*, **69**, 541–551.